Stable Haptic Interaction with Virtual Environments

Richard J. Adams, *Member, IEEE,* and Blake Hannaford, *Member, IEEE*

***Abstract*— A haptic interface is a kinesthetic link between a human operator and a virtual environment. This paper addresses fundamental stability and performance issues associated with haptic interaction. It generalizes and extends the concept of a virtual coupling network, an artificial link between the haptic display and a virtual world, to include both the impedance and admittance models of haptic interaction. A benchmark example exposes an important duality between these two cases. Linear circuit theory is used to develop necessary and sufficient conditions for the stability of a haptic simulation, assuming the human operator and virtual environment are passive. These equations lead to an explicit design procedure for virtual coupling networks which give maximum performance while guaranteeing stability. By decoupling the haptic display control problem from the design of virtual environments, the use of a virtual coupling network frees the developer of haptic-enabled virtual reality models from issues of mechanical stability.**

***Index Terms*—Absolute stability, force feedback, haptic interface, impedance control, two-port network, unconditional stability, virtual reality.**

I. Introduction

A haptic interface conveys a kinesthetic sense of presence to a human operator interacting with a computer generated environment. Historically, human-computer interaction has taken place through one-directional channels of information. Visual and audio information is sent from the computer to the operator. Keyboard, mouse, and joystick inputs transfer human inputs to the machine. Human neuromuscular and decision responses close this information loop. Oscillatory behavior is possible in this configuration, for example, when attempting to track a moving target with the mouse in the presence of delay in the rendering of graphics. Since there is no kinesthetic energy flow to the operator, such an event is at worst annoying, but never physically threatening. Haptic interaction is fundamentally different in that physical energy flows bi-directionally, from and to the human operator. The haptic display, typically some form of robotic manipulator, creates a feedback loop which includes not only the human neuromuscular and decision responses, but also the biomechanical impedance characteristics of the operator's contact with the device. The human grasp may stabilize an otherwise unstable system by absorbing mechanical energy. Conversely, the human grasp may destabilize an otherwise stable system by reflecting energy back into the system. Since the haptic device actively generates physical energy, instabilities can damage hardware and even pose a physical threat to the human.

A number of authors have considered issues of stability in haptic simulation. Minsky *et al.* [1] explored stability problems in the haptic display of simple virtual environments. They noted a critical tradeoff between simulation rate, virtual wall stiffness, and device viscosity and provided insights into the role of the human operator in stability concerns. A more rigorous examination of the stability problem was performed by Colgate *et al.* [2]. They used a simple benchmark problem to derive conditions under which a haptic display would exhibit passive behavior. Salcudean and Vlaar [3] studied the stability properties of a discrete, proportional-plus-derivative, virtual wall implementation for a magnetically levitated force feedback joystick. They found very low device friction significantly limited the achievable stiffness of the virtual environment. A much higher perceived stiffness was achieved using a braking pulse at the moment of impact with the virtual surface. While each of these works are significant contributions to the field, their analyzes are limited to specific assumptions about the type of haptic display used and the type of virtual environment being simulated. The problem lies in the fact that no distinction is made between the virtual environment and the control law for the haptic device. In fact, in the above examples, the virtual environment is the control law. It is encumbered with twin roles of creating realistic force feedback cues to render a virtual scene and ensuring the haptic device remains stable.

One way of decoupling the haptic device control problem from virtual scene generation is the introduction of an artificial coupling between the haptic display and the virtual environment. Colgate *et al.* [4] introduced the idea of a virtual coupling for haptic displays which guarantees stability for arbitrary passive human operators and environments. Zilles and Salisbury [5] presented a heuristically motivated "god-object" approach which greatly simplifies control law design. Ruspini *et al.* [6] use a virtual "proxy" extension of the god-object to couple a Phantom device to a three degree-of-freedom constraint based simulation. These implementations can be grouped together as special cases of a virtual coupling network, a two-port interface between the haptic display and the virtual environment. This network can play the important role of making the stability of the haptic simulation independent of both human grasp impedance and the details of virtual environment design. All of the above-mentioned work focuses on one particular class of haptic display, those which render impedance. No similar work on virtual couplings has appeared for the complementary case of haptic displays which render

Manuscript received December 1, 1997; revised January 15, 1999. This paper was recommended for publication by Associate Editor K. Kosuge and Editor S. Salcudean upon evaluation of the reviewers' comments. This paper was presented in part at the IEEE International Conference on Intelligent Robots and Systems, Victoria, B.C., Canada, October 15, 1998.

The authors are with the Department of Electrical Engineering, University of Washington, Seattle, WA 98195-2500 USA.

Publisher Item Identifier S 1042-296X(99)03547-8.

admittance and very little exists in explicit criteria for the design of virtual coupling networks.

This paper extends the concept of a virtual coupling to admittance displays and attempts to treat the problem of stable haptic interaction in a more general framework which encompasses any combination of haptic display and virtual environment causality. Llewelyn's criteria for "unconditional stability" is introduced as a tool in the design and evaluation of virtual coupling networks. A benchmark example illustrates some fundamental stability and performance tradeoffs and brings to light an important duality between the impedance and admittance models of haptic interaction.

II. Preliminaries

A. Terminology

The following terms are used throughout this paper.

Haptic display mechanical device configured to convey kinesthetic cues to a human operator.

Haptic displays vary greatly in kinematic structure, workspace, and force output. They can be broadly classified into two categories, those which "measure motion and display force" and those which "measure force and display motion" [7]. The former will be referred to as impedance displays, the latter as admittance displays. Impedance displays typically have low inertia and are highly back-drivable. The well known Phantom [8] family of haptic displays, the McGill University Pantograph [9], and the University of Washington Pen-Based Force Display [10] fall into this class, along with many others. Admittance displays are often high-inertia, non back-drivable manipulators fitted with force sensors and driven by a position or velocity control loop. Examples include Carnegie Mellon University's WYSIWYF Display [11] and the Iowa State/Boeing virtual aircraft control column [12], both of which are based upon PUMA 560 industrial robots.

Haptic interface includes everything that comes between the human operator and the virtual environment.

This always includes the haptic device, control software, and analog-to-digital/digital-to-analog conversion. It may also include a virtual coupling network which links the haptic display to the virtual world. The haptic interface characterizes the exchange of energy between the operator and the virtual world and thus is important for both stability and performance analysis.

Virtual environment computer generated model of some physically motivated scene.

The virtual world may be as elaborate as a high-fidelity walk-through simulation of a new aircraft design, or as simple as a computer air hockey game. Regardless of its complexity, there are two fundamentally different ways in which a physically based model can interact with the haptic interface. The environment can act as an impedance, accepting velocities (or positions) and generating forces according to some physical model. This class includes all so-called penalty based approaches and to-date has been the most prevalent [1]–[3], [8], [10]. The other possibility is for the virtual environment to act as an admittance, accepting forces and returning velocities (or positions). Included here are constraint based techniques. These approaches, already common in the computer science community, are now seeing application in haptic simulations [5], [13], [14].

Haptic simulation synthesis of human operator, haptic interface, and virtual environment which creates a kinesthetically immersive experience.

All of these elements are important in determining the stability of the system. The simulation includes continuous components, such as the human operator and mechanical device, as well as digital components, like the virtual world model and control software.

Causality structure choice of haptic display type (impedance or admittance) and virtual environment type (impedance or admittance), of which there are four possibilities.

Previous work has almost always focused on one of these four combinations, making results specific to that particular case.

B. Two-Port Characterizations

Two-port models, common in circuit theory, are a natural way of describing stability and performance in bilateral teleoperation [15], [16]. They have similar utility in haptic simulation for characterizing the exchange of energy between human operator, haptic interface, and virtual environment. A general two-port is a "black-box" which captures the relationship between *efforts* (forces F_1, F_2) and *flows* (velocities $v_1, -v_2$) at the two accessible terminal pairs. The negative sign on velocity, seen here and throughout the paper, is necessary to maintain consistency with the network formalism.

The relationship between efforts and flows is commonly described in terms of an *immittance matrix*. We will refer to a mapping between two vectors, $y = Pu$, as an *immittance mapping* if $y^T u = F_1 v_1 + F_2(-v_2)$. The matrix P is then considered an immittance matrix. Possible immittance matrices are the impedance matrix, Z, the admittance matrix, Y, the hybrid matrix, H, and the alternate hybrid matrix, G. In general, both the immittance matrices and their sub-components are frequency dependent functions

$$\begin{bmatrix} F_1 \\ F_2 \end{bmatrix} = \begin{bmatrix} z_{11} & z_{12} \\ z_{21} & z_{22} \end{bmatrix} \begin{bmatrix} v_1 \\ -v_2 \end{bmatrix} \tag{1}$$

$$\begin{bmatrix} v_1 \\ -v_2 \end{bmatrix} = \begin{bmatrix} y_{11} & y_{12} \\ y_{21} & y_{22} \end{bmatrix} \begin{bmatrix} F_1 \\ F_2 \end{bmatrix} \tag{2}$$

$$\begin{bmatrix} F_1 \\ -v_2 \end{bmatrix} = \begin{bmatrix} h_{11} & h_{12} \\ h_{21} & h_{22} \end{bmatrix} \begin{bmatrix} v_1 \\ F_2 \end{bmatrix} \tag{3}$$

$$\begin{bmatrix} v_1 \\ F_2 \end{bmatrix} = \begin{bmatrix} g_{11} & g_{12} \\ g_{21} & g_{22} \end{bmatrix} \begin{bmatrix} F_1 \\ -v_2 \end{bmatrix}. \tag{4}$$

C. Stability Concepts

The haptic interface can be represented as a two-port which characterizes the exchange of energy between a human

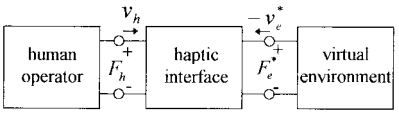

Fig. 1. A haptic simulation is made up of a haptic interface two-port with human operator and virtual environment one-port terminations.

operator (F_h, v_h) and a virtual environment $(F_e^*, -v_e^*)$. The star superscript indicates that a variable is discrete, it is otherwise assumed to be continuous. The haptic interface may, or may not, include a virtual coupling network. Fig. 1 shows the components of a haptic simulation.

The stability of a two-port depends on its terminal immittances. The immittance characteristics of the human operator can be represented either as an impedance, Z_h, or an admittance, Y_h. Likewise, the immittance properties of the virtual environment can be written as an impedance, Z_e, or an admittance, Y_e.

Definition 1: A continuous (discrete) linear two-port network with given terminal immittances is stable if and only if the corresponding characteristic equation has no roots in the right half s-plane (outside the unit circle, z-plane) and only simple roots on the imaginary axis (unit circle).

The haptic interface must be designed under the assumption that human operator and virtual environment behaviors are *a priori* unknown and potentially time varying. It is also likely that the virtual environment will be highly nonlinear. The stability problem must therefore be posed in terms of presumed levels of variation in the terminating port immittances. We will base stability arguments upon the assumption that the human operator and virtual environment are passive operators. There is reasonable precedence for treating human interaction with a robotic manipulator as passive [17]. Requiring that the virtual environment act as a passive operator is less sure. It is intuitive that the simulation of physically motivated effects (masses, springs, dampers) should obey conservation laws of physics, and thus be passive. However, formulating numerical integration routines which achieve strict adherence to these laws can be difficult. Fortunately, experience has shown that haptic interfaces designed under these assumptions are very robust when coupled to virtual environments which are "almost" passive [13], [18], [19]. The design of virtual environments which present a passive port to the haptic interface and the design of haptic interfaces which are robust to nonpassive virtual environments are subjects of ongoing research.

If a linear time-invariant (LTI) two-port can be shown to be passive, the system will be stable when coupled to an arbitrary network which is itself passive [20]. This provides a sufficient condition for the haptic interface stability problem.

Definition 2: A two-port is *passive* if and only if the immittance mapping $y = Pu$ satisfies

$$\int_0^t y^T(\tau)\mu(\tau)\, d\tau \geq 0 \quad \forall t \geq 0 \tag{5}$$

for all admissible efforts (F_1, F_2) and flows $(v_1, -v_2)$. For a linear network, this is equivalent to requiring that P be positive real.

Definition 3: The continuous (discrete) linear immittance matrix P is *positive real* if and only if P has no poles in the right half s-plane (outside the unit circle, z-plane), only simple poles on the imaginary axis (unit circle), and

$$P(j\omega) + P^T(-j\omega) \geq 0, \quad \forall \omega \geq 0. \tag{6}$$

The last condition can be further refined if we restrict our attention to two-port networks [21]

$$\begin{aligned} &\mathrm{Re}(p_{11}) \geq 0, \quad \mathrm{Re}(p_{22}) \geq 0 \\ &\mathrm{Re}(p_{11})\,\mathrm{Re}(p_{22}) - \left|\frac{p_{21}+p_{12}}{2}\right|^2 \geq 0, \quad \forall \omega \geq 0. \end{aligned} \tag{7}$$

Recall that for the haptic interface problem, we are interested only in one-port terminations of the haptic interface two-port by human operator and virtual environment immittances. Requiring that the haptic interface be passive can be conservative in this case, since it allows for arbitrary passive two-port terminations. A less conservative way of posing the stability problem for the haptic interface is in terms of "unconditional stability" [21].

Definition 4: A linear two-port is *unconditionally stable* if and only if there exists no set of passive terminating one-port immittances for which the system is unstable.

A passive network will always be unconditionally stable, but an unconditionally stable network is not necessarily passive. We will also make use of the term "potential instability."

Definition 5: A two-port network is *potentially unstable* if it is not unconditionally stable. For linear two-ports, Llewellyn's stability criteria provide both necessary and sufficient conditions for unconditional stability [22]

$$\begin{aligned} &\mathrm{Re}(p_{11}) \geq 0 \\ &2\,\mathrm{Re}(p_{11})\,\mathrm{Re}(p_{22}) \geq |p_{12}p_{21}| + \mathrm{Re}(p_{12}p_{21}), \quad \forall \omega \geq 0. \end{aligned} \tag{8}$$

Together, these two inequalities imply $\mathrm{Re}(p_{22}) \geq 0$.

Llewellyn's criteria may be equivalently applied to any of the four possible immittance forms (1)–(4). The satisfaction of (8) for one immittance form is necessary and sufficient for the satisfaction of (8) for the other three. In the special case of a network for which $h_{21} = -h_{12}$ (or equivalently $z_{21} = z_{12}$), the tests for passivity, (7), and for unconditional stability, (8), are identical. In this case, a network is said to be reciprocal [23].

For the problem at hand, unconditional stability means that the haptic interface must be stable for any set of passive human operators and virtual environments. In other words, the haptic interface will remain stable whether the operator holds it with a steel grip, or breaks contact completely. Simultaneously, the environment may simulate free or rigidly constrained motion. Llewellyn's criteria require that the haptic interface be LTI, at least locally. The human operator and virtual environment can be nonlinear and time-varying, as long as they are passive. Two-port unconditional stability is equivalent to the more general concept of $2n$-port "coupled stability" [20], [24]. Unfortunately, unlike the two-port case, coupled stability criteria for $2n$-ports are sufficient, but not necessary. Results may therefore be conservative. A $2n$-port

immittance matrix may be tested for coupled stability directly using a Popov-multiplier formulation [25], or by transforming it into scattering form through a bilinear transformation and then applying structured singular value analysis [26], [24].

D. Performance Concepts

The performance of a haptic interface can be described in terms of transparency, the quality in which velocities and forces are passed between the human operator and the virtual environment. A haptic interface with perfect transparency has the hybrid mapping [15]

$$\begin{bmatrix} F_h \\ -v_e^* \end{bmatrix} = \begin{bmatrix} 0 & 1 \\ -1 & 0 \end{bmatrix} \begin{bmatrix} v_h \\ F_e^* \end{bmatrix}. \tag{9}$$

Colgate and Brown [27] proposed using the Z-width as a measure of performance. The Z-width is defined as the achievable range of impedances which the haptic interface can stably present to the operator. This range is delimited by frequency dependent lower and upper bounds, $Z_{\min}$ and $Z_{\max}$. The ideal haptic interface could simulate free motion without inertia or friction, as well as infinitely rigid and massive objects. It will become evident later that perfect transparency and an infinite impedance range are unattainable and even undesirable goals.

E. Network Duality

A special relationship may exist between two networks which allows one network to be reconstructed from another using a simple substitution of variables.

Definition 6: Two networks, Ω_a and Ω_b, are said to be *dual* if for every admissible signal pair $[F_a, v_a] \in \Omega_a$, there exists an admissible signal pair $[F_b, v_b] \in \Omega_b$, such that $F_a = v_b$ and $F_b = v_b$. Likewise, for every admissible signal pair $[F_b, v_b] \in \Omega_b$, there exists an admissible signal pair $[F_a, v_a] \in \Omega_a$, such that $F_b = v_a$ and $F_a = v_b$ [29].

Frequently, the analysis of one network can be simplified by relating it to a better understood dual form. We will make use of this concept of duality in the analysis and design of haptic interfaces.

III. Benchmark Example

The following example, while simple, encompasses many of the most important factors which affect the stability and performance of haptic interfaces. These include open-loop device impedance, sample-hold effects, and, in the case of admittance displays, velocity loop bandwidth and closed-loop compliance. This benchmark problem reveals a number of fundamental issues in designing stable haptic interfaces and exposes an important duality between the impedance and admittance models of haptic interaction. We consider a one degree-of-freedom, rigid manipulator with mass m and damping b, shown in Fig. 2. This device is governed by the equations of motion

$$m\dot{v}_d + bv_d = F_h - F_d, \quad v_d = v_h. \tag{10}$$

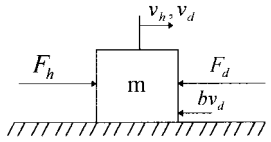

Fig. 2. Benchmark haptic display. The velocity of the human operator at the point of contact with the device is v_h. The velocity of the device at the point of actuation is v_d. The force, F_h, is applied to/by human operator at the point of contact. F_d is the force applied by/to the haptic device at the point of actuation.

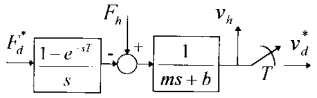

Fig. 3. Impedance display is discretized with a zero-order hold in the F_d path.

A. Impedance Display

In the impedance model of haptic interaction, forces are applied to the human operator in response to measured displacements. It is straightforward to form an impedance display from the equations of motion of our benchmark system. The corresponding hybrid mapping is

$$\begin{bmatrix} F_h \\ -v_d \end{bmatrix} = \begin{bmatrix} ms+b & 1 \\ -1 & 0 \end{bmatrix} \begin{bmatrix} v_h \\ F_d \end{bmatrix}. \tag{11}$$

1) Conventional Design: The causality structure best represented in the literature is impedance display/impedance environment [1]–[3], [8], [10]. One implementation of this structure is simply to set $v_d = v_e$ and $F_d = F_e$. The resulting continuous-time immittance matrix is reciprocal and satisfies both the conditions for passivity (7) and unconditional stability (8). We might be tempted to think our job is finished. To better understand the problem, sample-hold effects must be included. Fig. 3 shows the implementation of a sampled-data system using a zero-order hold at the force input and sampling the device velocity.

The open loop device dynamics are discretized using Tustin's method which preserves the passivity of the impedance function

$$Z_{d_I}(z) = (ms+b)|_{s \to (2/T)(z-1/z+1)}. \tag{12}$$

To maintain simplicity in the analysis, we assume that any aliasing effects due to sampling are negligible, thanks either to the low-pass filtering effect of device dynamics or the introduction of an appropriate anti-aliasing filter before sampling. The zero-order hold can then be approximated as a low-pass filter with a steady state gain of T and 90° phase lag at the Nyquist frequency. The sampler can be approximated as a static gain of $1/T$. With no loss of generality we can combine the sampler gain with the zero-order hold to get the normalized zero-order hold function

$$ZOH(z) = \frac{1}{2}\,\frac{(z+1)}{z}. \tag{13}$$

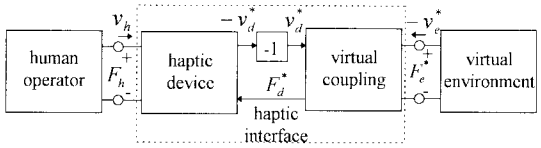

Fig. 4. Haptic interface for the impedance display case includes both the haptic display and a virtual coupling network.

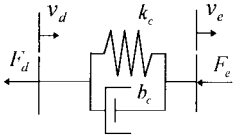

Fig. 5. Mechanical analog of a virtual coupling network.

We can now form the discrete hybrid matrix of the impedance display

$$\begin{bmatrix} F_h \\ -v_d^* \end{bmatrix} = \begin{bmatrix} Z_{d_I}(z) & ZOH(z) \\ -1 & 0 \end{bmatrix} \begin{bmatrix} v_h \\ F_d^* \end{bmatrix}. \tag{14}$$

Note that (14) is not reciprocal. We test the impedance display for unconditional stability by applying (8) to (14) to get

$$\frac{\mathrm{Re}(ZOH(z))}{|ZOH(z)|} \geq 1 \Leftrightarrow \cos(\angle ZOH(z)) \geq 1. \tag{15}$$

Since the zero-order hold (13) has a nonzero phase lag for $0 < \omega < 2\pi/T$, this condition is never satisfied. Thus, we see that, with $v_d^* = v_e^*$ and $F_d^* = F_e^*$, the haptic interface will never be unconditionally stable. This does not mean that the haptic simulation will necessarily be unstable, only that some combination of passive human operator and virtual environment exists that will destabilize the system. The biomechanical impedance properties of the human operator are unpredictable. The operator may decide to grasp the manipulator tightly, or release it altogether. It is difficult to guarantee stability when it is dependent on human operator behavior. We would therefore like to maintain a stable system for any level of human interaction, the only restriction being that the human operator is passive. In this conventional approach, it is left to the designer of the virtual environment to create a simulation which guarantees the stability of the haptic simulation. For complex virtual environments, this leads to a highly iterative tuning process which at best gives a conservative result. Since it is difficult to consider all possible events and configurations in a virtual world, even after this costly tuning procedure, there is no guarantee of stability. Additionally, this approach ties the design of the virtual environment to a specific haptic display. If a different display is coupled to the same environment, the system's stability properties change. This problem motivates the introduction of a virtual coupling network which guarantees the stability of a haptic interface when coupled with any passive virtual environment and human operator.

2) Proposed Design Procedure: We now specify the haptic interface to be the cascade combination of a haptic display and a virtual coupling network. Our goal becomes to design the virtual coupling network such that the combined system is unconditionally stable. Fig. 4 illustrates the concept.

In general, the virtual coupling network can have arbitrary structure. A physically motivated implementation is a spring-damper with stiffness, k_c, and damping, b_c, linking the haptic display to the virtual environment. Fig. 5 shows the mechanical analog of this coupling. If we simulate an infinitely stiff environmental constraint, the stiffness perceived by the human operator is not infinite, but that of the virtual coupling. An optimal stability-performance trade-off is achieved when virtual coupling stiffness is maximized, while preserving the unconditional stability of the combined two-port.

Discretization of virtual coupling impedance is performed using a first difference approximation

$$Z_{c_I}(z) = \left(b_c + \frac{k_c}{s}\right)\Big|_{s \to (z-1/Tz)} \tag{16}$$

The hybrid mapping of the virtual coupling network is

$$\begin{bmatrix} F_d^* \\ -v_e^* \end{bmatrix} = \begin{bmatrix} 0 & 1 \\ -1 & \dfrac{1}{Z_{c_I}(z)} \end{bmatrix} \begin{bmatrix} v_d^* \\ F_e^* \end{bmatrix}. \tag{17}$$

The hybrid mapping for the haptic interface is the cascade connection of the impedance display with the virtual coupling network

$$\begin{bmatrix} F_h \\ -v_e^* \end{bmatrix} = \begin{bmatrix} Z_{d_I}(z) & ZOH(z) \\ -1 & \dfrac{1}{Z_{c_I}(z)} \end{bmatrix} \begin{bmatrix} v_h \\ F_e^* \end{bmatrix}. \tag{18}$$

Note that the only change from (14) to (18) is the insertion of the virtual coupling term in the lower-right block. Directly applying (8), the criteria for unconditional stability are

$$\mathrm{Re}(Z_{d_I}(z)) \geq 0, \quad \mathrm{Re}(1/Z_{c_I}(z)) \geq 0 \tag{19}$$

and

$$\cos(\angle ZOH(z)) + \frac{2\,\mathrm{Re}(Z_{d_I}(z))\,\mathrm{Re}(1/Z_{c_I}(z))}{|ZOH(z)|} \geq 1. \tag{20}$$

We can make the following observations about (19) and (20).

1) $\mathrm{Re}(Z_{d_I}(z))$ can be interpreted as the physical damping of the impedance display. It must be nonzero and positive for unconditional stability to be possible. This is the level of damping the human operator feels when the virtual environment simulates free motion.
2) $\mathrm{Re}(1/Z_{c_I}(z))$ can be interpreted as the conductance of the virtual coupling. This function dictates the amount of "give" the human operator perceives in the haptic display when the virtual environment simulates a rigid constraint. Some minimum positive value of this "give" is necessary to achieve unconditional stability.
3) Larger values of $\mathrm{Re}(Z_{d_I}(z))$ permit smaller values of $\mathrm{Re}(1/Z_{c_I}(z))$. This means that increasing device damping increases the maximum impedance that can be presented to the human operator. If we want to simulate rigid contact, significant physical damping in the haptic device is required. This observation is consistent with those made by Brown and Colgate [27].
4) $\angle ZOH(z)$ is the phase loss due to sample-hold effects. Reducing the sampling frequency will cause an increase in this phase loss and require an augmentation in either

device damping or "give" in the virtual coupling to maintain unconditional stability.

Manipulating (20) gives us the following condition for unconditional stability:

$$\mathrm{Re}(1/Z_{c_I}(z)) \geq \frac{1-\cos(\angle ZOH(z))}{2\,\mathrm{Re}(Z_{d_I}(z))}\,|ZOH(z)|. \quad (21)$$

Both sides of this inequality are functions of frequency. We now have a design procedure for the virtual coupling network. Plot the right-hand side of (21) versus frequency, then synthesize $1/Z_{c_I}(z)$ so that its real part is positive and exceeds this lower-bound.

Note that if the inequality (21) holds, unconditional stability is satisfied, regardless of whether an impedance or admittance type virtual environment is used. The only difference is in the implementation. The hybrid mapping of the virtual coupling network, (17), links the haptic display to the virtual environment in the impedance display/impedance environment case. If the virtual environment is modeled as an admittance, the case when using constraint based simulations, the same virtual coupling is implemented as

$$\begin{bmatrix} F_d^* \\ F_e^* \end{bmatrix} = \begin{bmatrix} Z_{c_I}(z) & Z_{c_I}(z) \\ Z_{c_I}(z) & Z_{c_I}(z) \end{bmatrix} \begin{bmatrix} v_d^* \\ -v_e^* \end{bmatrix}. \quad (22)$$

We can therefore design the haptic interface without considering the virtual environment implementation, as long as it is passive. An interesting note is that a virtual coupling will always be needed to implement dissimilar causality structures. Without a coupling network, an impedance display must be paired with an impedance environment. Likewise, an admittance display could only be used with an admittance environment. The virtual coupling network permits all four causality structures to be used.

The hybrid matrix of the combined haptic interface network, (18), illustrates that to best approximate perfect transparency, (9), $Z_{c_I}(z)$ should be as large as possible. This means for performance, we want high virtual stiffness and virtual damping. The best virtual coupling is therefore one that makes (21) an equality, providing the minimum level of compliance for unconditional stability. The performance of the haptic interface can be quantified in terms of lower and upper bounds on the impedance perceived by the human operator, Z_P. By terminating the virtual environment port of (18), $F_e^* = Z_e v_e^*$, we can calculate the resulting one-port impedance function

$$Z_P = \frac{F_h}{v_h} = Z_{d_I}(z) + \frac{Z_{c_I}(z)ZOH(z)Z_e}{Z_{c_I}(z)+Z_e}. \quad (23)$$

This is the impedance felt by the human operator for a given virtual environment, Z_e. The lower bound on Z-width is calculated by letting $Z_e \to 0$. The minimum impedance that an impedance-type haptic device can simulate is limited by its open-loop inertia and friction

$$Z_{\min_I} = Z_{d_I}(z). \quad (24)$$

The upper bound is calculated by letting $Z_e \to \infty$. The resulting maximum impedance is the impedance of the open-loop device plus that of the virtual coupling

$$Z_{\max_I} = Z_{d_I}(z) + Z_{c_I}(z)ZOH(z). \quad (25)$$

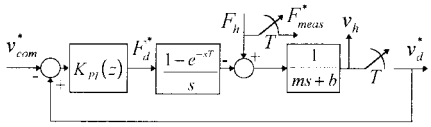

Fig. 6. Admittance display includes a velocity control loop, discretized with a zero-order hold in the F_d path.

The two functions, $Z_{\min_I}$ and $Z_{\max_I}$, define the Z-width of the haptic interface. We can combine (24) and (25) to get

$$Z_{\max_I} = Z_{\min_I} + Z_{c_I}(z)ZOH(z). \quad (26)$$

This implies that to maximize Z-width, we should maximize virtual coupling impedance, or equivalently, minimize virtual coupling compliance.

B. Admittance Display

In the admittance model of haptic interaction, the display generates displacements in response to measured forces. We can derive such a display by adding a proportional-plus-integral (PI) velocity control loop,

$$F_d^* = K_{\mathrm{PI}}(z)(v_d^* - v_{\mathrm{com}}^*) \quad (27)$$

and measuring force at the point of device-human contact. Note that PI feedback of velocity is equivalent to proportional-plus-derivative feedback of position. The PI form is used here for consistency in notation. v_{com}^* is the commanded velocity and F_{meas}^* is the measured force. The admittance display is implemented according to Fig. 6. The resulting alternate hybrid mapping for the discretized display is

$$\begin{bmatrix} v_h \\ F_{\mathrm{meas}}^* \end{bmatrix} = \begin{bmatrix} \dfrac{1}{Z_{d_A}(z)} & -T(z) \\ 1 & 0 \end{bmatrix} \begin{bmatrix} F_h \\ -v_{\mathrm{com}}^* \end{bmatrix} \quad (28)$$

where

$$T(z) = \frac{ZOH(z)K_{\mathrm{PI}}(z)}{Z_{d_I}(z) + ZOH(z)K_{\mathrm{PI}}(z)} \quad (29)$$

is the complementary sensitivity function which represents the ability of the velocity loop to track commands and

$$Z_{d_A}(z) = Z_{d_I}(z) + K_{\mathrm{PI}}(z)ZOH(z) \quad (30)$$

is the driving-point impedance of the admittance display at the human operator port.

We can now make a very important observation. The network representation of the admittance display, (28), has a dual relationship to the network form of the impedance display, (14). Forces map to velocities, velocities map to forces, impedance functions map to admittance functions, and force transfer functions map to velocity transfer functions. This duality is useful when considering system stability and the design of virtual coupling networks.

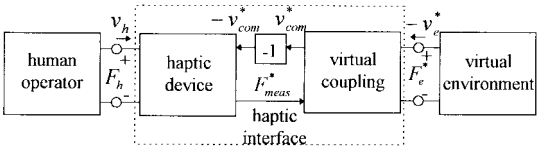

Fig. 7. Haptic interface for the admittance display case includes both the haptic display and a virtual coupling network.

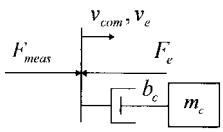

Fig. 8. Simple virtual coupling network for an admittance display.

1) Conventional Design: A simple admittance/admittance causality structure can be implemented without a virtual coupling by setting $v^*_{\rm com} = v^*_e$ and $F^*_{\rm meas} = F^*_e$. Is the resulting two-port passive? For this system, it is convenient to use the alternate hybrid matrix to check for unconditional stability (28). The result is

$$\frac{\mathrm{Re}(T(z))}{|T(z)|} \geq 1 \Leftrightarrow \cos(\angle T(z)) \geq 1. \tag{31}$$

Since $\cos(\angle T(z)) < 1$ for any amount of lead or lag between the commanded and realized velocity, the admittance display is never unconditionally stable.

2) Proposed Design Procedure: Our goal is to design a virtual coupling network such that the combined haptic interface network with an admittance display is unconditionally stable. Fig. 7 shows the combined system.

The choice of a virtual coupling function is not intuitive in this case. We know that in a network sense, the admittance display is the dual of the impedance display. It follows that the coupling for the admittance display should be the dual of the impedance display virtual coupling network. The mechanical dual of the parallel spring-damper in Fig. 5 is a series mass-damper combination. Fig. 8 shows a free-body-diagram of this coupling scheme. In this case, the virtual coupling aims to provide some minimum level of impedance for the virtual environment. It limits the degree to which the haptic interface can simulate free motion. The chosen coupling can be thought of as a frequency-dependent damper. It has zero steady-state resistance. At high-frequencies, the impedance of the mass becomes dominant, creating an effective damping of b_c. The admittance function of the virtual coupling is

$$Y_{c_A}(z) = \left(\frac{1}{b_c} + \frac{1}{m_c s}\right)\Big|_{s \to (z-1/Tz)}. \tag{32}$$

The corresponding impedance function is $Z_{c_A}(z) = 1/Y_{c_A}(z)$. With the coupling in place, the human operator will always feel some level of viscosity and inertia in the haptic interface, even when the virtual environment simulates free motion. The best stability/performance trade-off is achieved when coupling impedance is set to the minimum level which makes the combined two-port unconditionally stable.

The alternate hybrid form of the virtual coupling network is

$$\begin{bmatrix} v^*_{\rm com} \\ F^*_e \end{bmatrix} = \begin{bmatrix} 0 & -1 \\ 1 & Z_{c_A}(z) \end{bmatrix} \begin{bmatrix} F^*_{\rm meas} \\ -v^*_e \end{bmatrix}. \tag{33}$$

The alternate hybrid mapping for the combined haptic interface network then becomes

$$\begin{bmatrix} v_h \\ F^*_e \end{bmatrix} = \begin{bmatrix} \dfrac{1}{Z_{d_A}(z)} & -T(z) \\ 1 & Z_{c_A}(z) \end{bmatrix} \begin{bmatrix} F_h \\ -v^*_e \end{bmatrix}. \tag{34}$$

With the virtual coupling in place, only the lower-right term has changed in the alternate hybrid matrix from (28) to (34). For unconditional stability, the necessary and sufficient conditions are

$$\mathrm{Re}(Z_{c_A}(z)) \geq 0, \quad \mathrm{Re}(1/Z_{d_A}(z)) \geq 0 \tag{35}$$

and

$$\cos(\angle T(z)) + \frac{2\,\mathrm{Re}(Z_{c_A}(z))\,\mathrm{Re}(1/Z_{d_A}(z))}{|T(z)|} \geq 1. \tag{36}$$

We can make the following observations about (35) and (36).

1) $\mathrm{Re}(Z_{c_A}(z))$ can be interpreted as the damping of the virtual coupling. It must be nonzero and positive for unconditional stability to be possible. This damping is what the human operator feels when the virtual environment simulates free motion.
2) $\mathrm{Re}(1/Z_{c_A}(z))$ can be interpreted as the conductance of the admittance display. This function dictates the amount of "give" the human operator perceives in the haptic display when the virtual environment simulates a rigid constraint. Some minimum positive value is necessary to achieve unconditional stability. The need for compliance in an admittance implementation was previously observed by Kazerooni in his work on man-extenders [28].
3) Larger values of $\mathrm{Re}(1/Z_{d_A}(z))$ permit smaller values of $\mathrm{Re}(Z_{c_A}(z))$. This means that reducing the inner loop gains, $K_{\rm PI}(z)$, improves the ability of the haptic interface to simulate free motion. At the same time, high values of $Z_{\rm PI}(z)$ are desirable to simulate rigid constraints. The inner loop control must be chosen to strike a trade-off between these conflicting requirements.

Manipulating (36) gives us the following condition for unconditional stability:

$$\mathrm{Re}(Z_{c_A}(z)) \geq \frac{1-\cos(\angle T(z))}{2\,\mathrm{Re}(1/Z_{d_A}(z))}\,|T(z)|. \tag{37}$$

A design procedure for the virtual coupling network is to plot the right-hand side of (37) versus frequency, then synthesize $Z_{c_A}(z)$ so that its real part is positive and exceeds this lower-bound.

As before, unconditional stability is satisfied as long as (37) holds, regardless of whether an impedance or admittance type environment is used. The alternate hybrid mapping of the virtual coupling network, (33), links the haptic display to an

admittance environment. For an impedance environment, the virtual coupling is implemented as

$$\begin{bmatrix} v^*_{\text{com}} \\ -v^*_e \end{bmatrix} = \begin{bmatrix} \dfrac{1}{Z_{c_A}(z)} & -\dfrac{1}{Z_{c_A}(z)} \\ -\dfrac{1}{Z_{c_A}(z)} & \dfrac{1}{Z_{c_A}(z)} \end{bmatrix} \begin{bmatrix} F^*_{\text{meas}} \\ F^*_e \end{bmatrix}. \tag{38}$$

The alternate hybrid matrix of the combined haptic interface network, (34), shows that to maximize transparency, $Z_{c_A}(z)$ should be as small as possible. In other words, for performance, we want low virtual damping. The best virtual coupling network is thus one that minimally exceeds the lower-bound for unconditional stability. The performance of the admittance implementation can be analyzed by terminating the virtual environment port of (34) with $v^*_e = Y_e F^*_e$. The resulting one-port function, Y_P

$$Y_P = \frac{v_h}{F_h} = 1/Z_{d_A}(z) + \frac{T(z)Y_e}{1 + Z_{c_A}(z)Y_e} \tag{39}$$

represents the admittance perceived by the human operator for a given virtual environment. The minimum admittance which can be simulated by the haptic interface is found by letting $Y_e \rightarrow 0$

$$Y_{\min_A} = 1/Z_{d_A}(z). \tag{40}$$

The maximum admittance is calculated by letting $Y_e \rightarrow \infty$

$$Y_{\max_A} = 1/Z_{d_A}(z) + T(z)/Z_{c_A}(z). \tag{41}$$

The lower bound on Z-width is the inverse of maximum admittance

$$Z_{\min_A} = \frac{Z_{c_A}(z)}{T(z) + Z_{c_A}(z)/Z_{d_A}(z)}. \tag{42}$$

The upper bound on Z-width is the inverse of the minimum admittance function

$$Z_{\max_A} = Z_{d_A}(z) = Z_{d_I}(z) + K_{\text{PI}}(z)ZOH(z). \tag{43}$$

We see that high gains in the velocity tracking control law, $K_{\text{PI}}(z)$, are needed to increase $Z_{\max_A}$ and better simulate rigid constraints. We observed earlier that to achieve unconditional stability and low impedance motion, $K_{\text{PI}}(z)$ must be small. We are faced with a trade-off between performance when simulating free motion [small $Z_{\min_A}$, small $K_{\text{PI}}(z)$] and performance when simulating rigid objects [large $Z_{\max_A}$, large $K_{\text{PI}}(z)$].

IV. Duality

The impedance display two-port network, (14), is the dual of the admittance display two-port, (28). Similarly, the virtual coupling networks, (17) and (33), are dual, and the combined haptic interface networks, (18) and (34), for the two cases are dual. The correspondence of parameters is shown in Table I. The impedance matrix in one case is the dual mapping of the admittance matrix in the other, and the hybrid matrix is the dual mapping of the alternate hybrid matrix. This strong relationship between the two cases provides a number of interesting insights into stability problems.

TABLE I
Correspondance in Impedance/Admittance Display Duality

Impedance Display		Admittance Display
$Z_{d_I}(z)$	$\leftrightarrow$	$1/Z_{d_A}(z)$
$1/Z_{c_I}(z)$	$\leftrightarrow$	$Z_{c_A}(z)$
$ZOH(z)$	$\leftrightarrow$	$T(z)$

1) We observed earlier that a minimum level of damping was needed in the impedance display to guarantee unconditional stability. Duality maps this requirement to the need for a minimum level of compliance in the admittance display

$$\text{Re}(Z_{d_I}(z)) \geq 0 \leftrightarrow \text{Re}(1/Z_{d_A}(z)) \geq 0. \tag{44}$$

2) For the impedance display, we have seen that the virtual coupling must have a minimum level of compliance for the haptic interface to be unconditional stable. Duality maps this requirement to the need for a minimum level of impedance in the virtual coupling of the admittance display

$$\text{Re}(1/Z_{c_I}(z)) \geq 0 \leftrightarrow \text{Re}(Z_{c_A}(z)) \geq 0. \tag{45}$$

3) The zero-order hold approximation and the velocity tracking function are dimensionless mappings which have similar effects on stability for their respective cases. $ZOH(z)$ represents the ability of the impedance display to display environmental forces to the human operator when $v_h = 0$. $T(z)$ represents the ability of the admittance display to display environmental velocities when $F_h = 0$.
4) Worst case stability for the impedance implementation typically occurs when human operator impedance is low (loose grasp or hands-off) and virtual environment impedance is high (rigid constraint). Worst case stability for the admittance implementation normally occurs when human operator impedance is high (rigid grasp) and virtual environment impedance is low (free motion).

V. Discussion

The virtual coupling impedance functions, $Z_{c_I}(z)$ and $Z_{c_A}(z)$, restrict the impedance range which the haptic interface can present to the human operator and, in doing so, guarantee unconditional stability. $Z_{c_I}(z)$ generates an upper-bound on the maximum impedance of the impedance display, while $Z_{c_A}(z)$ creates a lower-bound on the minimum impedance of the admittance display. As mentioned earlier, the best choices for these functions are ones that satisfy (21) and (37) as equalities. The physically motivated virtual couplings mentioned in this paper may be conservative. Higher-order realizations, synthesized without any obvious physical analog, will potentially provide increased performance.

The benchmark example does not consider velocity estimation effects or structural flexibility in the haptic device. Following similar arguments, equivalent conditions to (21) and

(37) can be derived which include these issues [19]. They are omitted here for clarity of presentation and discussion. Adding complexity to the model does not change the fundamental relationships and tradeoffs described in this paper. For the same reasons, we have not included possible permutations on impedance and admittance display implementations, such as reducing the apparent device damping with positive velocity feedback. We have also limited the problem to a single degree-of-freedom device. This allows us to find necessary and sufficient conditions for unconditional stability and develop explicit design criteria for virtual coupling networks. Additional axes of motion can be handled with this approach if they are orthogonal or if they can be transformed into an orthogonal system. Otherwise, we must consider a $2n$-port representation of the haptic interface, instead of the two-port form used in this paper. A virtual coupling network may still be designed for individual axes using our approach, but post-design analysis using the methods described in [24] or [25] will be needed to guarantee unconditional stability.

While stability conditions based on the invariant stability factor are necessary and sufficient, they may still provide conservative results. The human operator is assumed to be passive, but passive functions can have infinitely high gain at high frequencies. The human grasp admittance function inherently has low-pass properties. A high-frequency violation of (21) or (37) may therefore be tolerable if additional analysis verifies that it corresponds to an unrealistically high impedance at the human operator port.

VI. Conclusion

The two-port mapping of network theory provides a framework for the unification of different models of haptic interaction. Four possible causality structures can be formed by selecting either an impedance or admittance display and an impedance or admittance virtual environment model. The introduction of a virtual coupling network between the mechanical device and the virtual environment guarantees the stability of the combined haptic interface for arbitrary passive human operator and environmental impedances. Necessary and sufficient conditions, based on Llewellyn's stability criteria, lead to an explicit procedure for the design of such couplings. We find that if the virtual environment is passive, the virtual coupling network design is independent of the impedance or admittance causality of the virtual environment model. In addition, the two-port network which arises in admittance display implementation and that which arises in impedance display implementation are dual. The unification of these different cases creates important insights into stability and performance for kinesthetic interaction with virtual worlds.

Perhaps the most significant benefit of the proposed approach to haptic interface design is that it decouples the haptic display control problem from the synthesis of virtual environments. An unconditionally stable haptic interface, whether based on a PUMA or a Phantom device, will stably interact with any passive virtual environment, be it penalty or constraint based. This natural separation of hardware and software is an important step in the growth of haptics as an industry. It will allow innovative businesses and individuals to build devices and write software that are compatible and safe.

References

[1] M. Minsky, M. Ouh-Young, O. Steele, F. P. Brooks, and M. Behensky, "Feeling and seeing issues in force display," *Comput. Graph.*, vol. 24, no. 2., pp. 235–243, 1990.

[2] J. E. Colgate, P. E. Grafing, M. C. Stanley, and G. Schenkel, "Implementation of stiff virtual walls in force-reflecting interfaces," in *Proc. IEEE Virtual Reality Annu. Int. Symp.*, Seattle, 1993, pp. 202–208.

[3] S. E. Salcudean, and T. D. Vlaar, "On the emulation of stiff walls and static friction with a magnetically levitated input/output device," *Trans. ASME J. Dyn. Syst., Meas., Contr.*, vol. 119, no. 1, pp. 127–132, 1997.

[4] J. E. Colgate, M. C. Stanley, and J. M. Brown, "Issues in the haptic display of tool use," in *Proc. IEEE/RSJ Int. Conf. Intell. Robots Syst.*, Pittsburgh, PA, 1995, pp. 140–145.

[5] C. B. Zilles and J. K. Salisbury, "A constraint-based God-object method for haptic display," in *Proc. IEEE/RSJ Int. Conf. Intell. Robots Syst.*, Pittsburgh, PA, 1995, pp. 146–151.

[6] D. C. Ruspini, K. Kolarov, and O. Khatib, "The Haptic display of complex graphical environments," in *Proc. Comput. Graphics SIGGRAPH '97*, Los Angeles, CA, 1997, pp. 345–352.

[7] T. Yoshikawa, Y. Yokokohji, T. Matsumoto, and X.-Z. Zheng, "Display of feel for the manipulation of dynamic virtual objects," *Trans. ASME J. Dyn. Syst., Meas., Contr.*, vol. 117, no. 4, pp. 554–558, 1995.

[8] T. H. Massie and J. K. Salisbury, "The phantom Haptic interface: A device for probing virtual objects," in *Proc. ASME Int. Mech. Eng. Congr. Exhibition*, Chicago, IL, 1994, pp. 295–302.

[9] V. Hayward, J. Choksi, G. Lanvin, and C. Ramstein, "Design and multi-objective optimization of a linkage for a Haptic interface," *Advances in Robot Kinematics and Computational Geometry*. Boston, MA: Kluwer, 1994, pp. 352–359.

[10] P. Buttolo and B. Hannaford, "Pen based force display for precision manipulation of virtual environments," in *Proc. IEEE Virtual Reality Annu. Int. Symp.*, Raleigh, NC, 1995, pp. 217–225.

[11] Y. Yokokohji, R. L. Hollis, and T. Kanade, "What you see is what you can feel-development of a visual/Haptic interface to virtual environment," in *Proc. IEEE Virtual Reality Annu. Int. Symp.*, Los Alamitos, CA, 1996, pp. 46–53.

[12] C. L. Clover, G. R. Luecke, J. J. Troy, and W. A. McNeely, "Dynamic simulations of virtual mechanisms with Haptic feedback using industrial robotics equipment," *Proc. IEEE Int. Conf. Robot. Automat.*, Albuquerque, NM, 1997, pp. 3205–3210.

[13] B. Chang and J. E. Colgate, "Real-time impulse-based simulation of rigid body systems for Haptic display," in *Proc. ASME Int. Mech. Eng. Congr. Exh.*, Dallas, TX, 1997, pp. 145–152.

[14] P. J. Berkelman and R. L. Hollis, "Haptic interaction using magnetic levitation," in *Proc. ASME Int. Mech. Eng. Congr. Exh.*, Anaheim, CA, 1998, pp. 187–188.

[15] B. Hannaford, "A design framework for teleoperators with kinesthetic feedback," *IEEE J. Robot. Automat.*, vol. 5, pp. 426–434, Aug. 1989.

[16] R. J. Anderson and M. W. Spong, "Asymptotic stability for force reflecting teleoperators with time delay," *Int. J. Robot. Res.*, vol. 11, no. 2, pp. 135–149, 1992.

[17] N. Hogan, "Controlling impedance at the man/machine," in *Proc. IEEE Int. Conf. Robot. Automat.*, Scottsdale, AZ, 1989, pp. 1626–1631.

[18] J. M. Brown and J. E. Colgate, "Minimum mass for Haptic display simulations," in *Proc. ASME Int. Mech. Eng. Congr. Exh.*, Anaheim, CA, 1998, pp. 249–256.

[19] R. J. Adams, M. R. Moreyra, and B. Hannaford, "Stability and performance of Haptic displays: Theory and experiments," in *Proc. ASME Int. Mech. Eng. Congr. Exh.*, Anaheim, CA, 1998, pp. 227–234.

[20] J. E. Colgate, "Coupled stability of multiport systems-theory and experiments," *Trans. ASME, J. Dyn. Syst., Meas., Contr.*, vol. 116, no. 3, pp. 419–428, 1994.

[21] E. F. Bolinder, "Survey of some properties of linear networks," *IRE Trans. Circuit Theory*, vol. CT-4, pp. 70–78, 1957.

[22] F. B. Llewellyn, "Some fundamental properties of transmission systems," *Proc. IRE*, vol. 40, pp. 271–283, 1952.

[23] S. S. Haykin, *Active Network Theory*. London, U.K.: Addison-Wesley, 1970.

[24] J. E. Colgate, "Robust impedance shaping telemanipulation," *IEEE Trans. Robot. Automat.*, vol. 9, pp. 374–384, Aug. 1993.

[25] J. H. Ly, M. G. Safonov, and R. Y. Chiang, "Real/complex multivarible stability margin computation via generalized Popov multiplier-LMI approach," in *Proc. ACC*, Baltimore, MD, 1994, pp. 425–429.

[26] J. C. Doyle, "Analysis of feedback systems with structured uncertainty," in *Proc. Inst. Elect. Eng. D*, 1982, vol. 129, no. 6, pp. 242–250.
[27] J. E. Colgate and J. M. Brown, "Factors affecting the Z-width of a Haptic display," in *Proc. IEEE Int. Conf. Robot. Automat.*, Los Alamitos, CA, 1994, pp. 3205–3210.
[28] H. Kazerooni, "Human/robot interaction via the transfer of power and information signals, Part I: Dynamics and control analysis," in *Proc. IEEE Int. Conf. Robot. Automat.*, Scottsdale, AZ, 1989, pp. 1632–1640.
[29] E. S. Kuh and R. A. Rohrer, *Theory of Linear Active Networks*. San Francisco, CA: Holden-Day, 1967.

Richard J. Adams (M'98) received the B.S. degree from the United States Air Force Academy, Colorado Springs, CO, in 1989, and the M.S. degree in aeronautics and astronautics from the University of Washington, Seattle, in 1990, where he is currently pursuing the Ph.D. degree in electrical engineering.

He is a Captain in the United States Air Force. After receiving the M.S. degree he worked the following three years in Wright Laboratory, Dayton, OH, on advanced flight controls for fighter aircraft. He recently served two years as an Exchange Scientist with the C.E.R.T. Research Center, Toulouse, France.

Capt. Adams received the Air Force Scientific Achievement Award for his work on F-16 high angle-of-attack control in 1994.

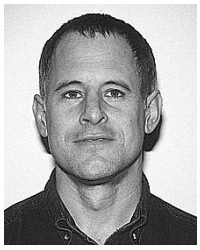

Blake Hannaford (S'82–M'85) received the B.S. degree in engineering and applied science from Yale University, New Haven, CT, in 1977, and the M.S. and Ph.D. degrees in electrical engineering from the University of California, Berkeley, in 1982 and 1985, respectively.

Before graduate study, he held engineering positions in digital hardware and software design, office automation, and medical image processing. At Berkeley, he pursued his thesis research in multiple target tracking in medical images and the control of time-optimal voluntary human movement. From 1986 to 1989, he worked on the remote control of robot manipulators in the Man-Machine Systems Group, Automated Systems Section, NASA Jet Propulsion Laboratory, California Institute of Technology, Pasadena, which he supervised from 1988 to 1989. Since September 1989, he has been at the University of Washington, Seattle, where he has been Associate Professor of Electrical Engineering since 1993. His interests include haptic displays on the internet, surgical biomechanics, and biologically based design of robot manipulators.

Dr. Hannaford received the National Science Foundation's Presidential Young Investigator Award and the Early Career Achievement Award from the IEEE Engineering in Medicine and Biology Society.